Journal of Solid State Chemistry **151,** 225–230 (2000)
doi:10.1006/jssc.2000.8644, available online at http://www.idealibrary.com on IDEAL®

Intercalates of Vanadyl and Niobyl Phosphates with C_4 Diols

Ludvík Beneš, Klára Melánová, and Vítězslav Zima

Joint Laboratory of Solid State Chemistry of the Academy of Sciences of the Czech Republic and University of Pardubice, Studentská 84, 532 10 Pardubice, Czech Republic
E-mail: ludvik.benes@upce.cz

Received October 5, 1999; in revised form January 31, 2000; accepted February 3, 2000

Intercalates of vanadyl and niobyl phosphates with 1,2-butanediol, 1,3-butanediol, 2,3-butanediol, 1,4-butanediol, *cis*-2-butene-1,4-diol, and 2-butyne-1,4-diol were prepared and characterized by XRD, TGA, and IR spectroscopy. Their thermal stability and stability in air were studied by XRD. Intercalates of both hosts with 1,4-butanediol and *cis*-2-butene-1,4-diol change into relatively stable phases with lower basal spacing during heating. $VOPO_4$ intercalated with 1,3-butanediol forms a Hendricks–Teller disordered structure in a wide temperature range.

Key Words: **intercalation; vanadyl phosphate; niobyl phosphate; diols.**

INTRODUCTION

Intercalation of various molecules into inorganic layered structures leads to new materials with interesting properties and structures. In recently published articles (1, 2) we have shown that the reaction of vanadyl and niobyl phosphates with 1,ω-alkanediols produces layer-type complexes of the formula $MOPO_4 \cdot C_nH_{2n}(OH)_2$ ($M = \mathrm{V, Nb}$; $n = 2$–10). The structure of these complexes retains planar $(MOPO_4)_\infty$ layers present in the original hosts. The intercalated diols are arranged in a monomolecular way between the host layers. One half of OH groups of the guest diol molecules is bound to the host layers by means of donor–acceptor O_{diol}–M_{host} bonds. The other OH groups are anchored to the host layers by a system of hydrogen bonds $(O{-}H)_{\mathrm{diol}} \cdots O_{\mathrm{host}}$. The carbon chains of the diols are probably in an all-*trans* conformation. The diol molecules are perpendicular to the layers in the vanadyl phosphate intercalates and tilted at an angle of 74° in the niobyl phosphate intercalates.

On the other hand, the 1,2-alkanediols molecules are arranged between the $(MOPO_4)_\infty$ layers in a bimolecular way with their aliphatic chains tilted at an angle of 70° (3). It was found that the intercalates contain 1.5 molecules of diol per formula unit. Three ways of bonding of the 1,2-alkanediol molecules to the host layers were proposed. Two molecules of diol are coordinated to the metal atoms by their first and second oxygen, respectively. The third diol molecule is anchored in the interlayer space by hydrogen bonds.

This present report summarizes studies of intercalation of butanediols with various positions of the OH groups and unsaturated C_4 diols into vanadyl and niobyl phosphates.

EXPERIMENTAL

1. *Preparations*

Vanadyl phosphate dihydrate and niobyl phosphate trihydrate were synthesized as previously described (4, 5). Intercalates of both hosts with all the diols studied were prepared by a reintercalation reaction. The solid propanol intercalated hosts (1, 2) were first prepared and used as a starting material for the reactions with the diols. Intercalates of $VOPO_4$ were obtained by a long-lasting contact of $VOPO_4 \cdot 2C_3H_7OH$ with an ether or acetonitrile solution of the corresponding diol. The intercalates of $NbOPO_4$ were prepared by suspending microcrystalline $NbOPO_4 \cdot 2C_3H_7OH$ in dry diol. This reaction mixture was exposed to a microwave field for about 10 min. The solid product formed was filtered off. All samples for X-ray diffraction analyses were left with a small residue of the respective diol to prevent decomposition. The samples for TG-DTA and elemental analyses were washed with dry acetonitrile or diethylether and dried at room temperature in nitrogen.

2. *Characterization of Intercalates*

The powder data of the intercalates with a minor surplus of the guest diol were obtained with an X-ray diffractometer (HZG-4, Germany) using Cu$K\alpha1$ radiation ($\lambda = 1.54051$ Å) with discrimination of the Cu$K\beta$ by a Ni-filter. The Cu$K\alpha2$ intensities were removed from the original data. Silicon ($a = 5.43055$ Å) was used as internal standard. Diffraction angles were measured from 3° to 37° (2Θ). Temperature

0022-4596/00 $35.00

measurements (from 22 to 240°C) were carried out on a heated corundum plate with a thermocouple (6). Each diffractogram was measured at constant temperature and a cycle of heating and measuring lasted about 20 min.

The TGAs of the intercalates were performed with a Derivatograph MOM (Hungary), the measurements being carried out in the temperature interval of 30–600°C in air at a heating rate of 5°C/min. The weight of the samples was 100 mg. In some cases, the composition was determined by elemental analysis (C, H).

Infrared spectra were recorded on a Bio-Rad FTS spectrometer with spectral range 4000–500 cm^{-1} using a dry KBr powder containing 10% of the intercalate. The resultant reflectance spectra were converted into Kubelka–Munk format.

3. X-Ray Diffraction of a Hendricks–Teller Disordered Layered Lattice

Layered crystals are not completely ordered in some cases. One type of disorder may be defined as a random irregular sequence of layers of different kinds. This irregularity leads to variation of diffraction angles and linewidths of interferences in the X-ray diffraction pattern (7). We can use the Hendricks–Teller theory for the description of this phenomenon if the following conditions are presumed: (i) only two types of layers are present with interlayer distances d_1 and d_2, (ii) both layers have the same structure factor, (iii) fractions f_1 and f_2 correspond to interlayer distances d_1 and d_2, respectively, (iv) geometric factors in the X-ray experiment are not considered, (v) thermal factors are neglected. Under these assumptions, the scattered intensity on Bragg angle may be described by (7)

$$I_{\mathrm{av}} = |V_{\mathrm{L}}|^2 \frac{1 - C^2}{1 - 2C\cos\Phi}, \qquad [1]$$

where I_{av} is the average scattered intensity per layer, V_{L} is the layer form factor, and

$$C = f_1 \cos(\Phi_1 - \bar{\Phi}) + f_2 \cos(\Phi_2 - \bar{\Phi}), \qquad [2]$$

where

$$\bar{\Phi} = \arctan\frac{f_1 \sin\Phi_1 + f_2 \sin\Phi_2}{f_1 \cos\Phi_1 + f_2 \cos\Phi_2} \qquad [3]$$

and

$$\Phi_i = \frac{4\pi d_i}{\lambda}\sin\Theta, \qquad [4]$$

where $i = 1$ or 2 respectively, and d_i is interlayer distance. A slight dependence of the layer form factor V_{L} on the diffraction angle Θ does not affect the computed basal plane linewidths and positions. The main term determining the positions, line shapes, and widths is $I_{\mathrm{av}}/|V_{\mathrm{L}}|^2$ in Eq. [1]. Three independent variables d_1, d_2, and f_1 are contained in this equation. The linewidths computed by this method correspond to disorder of layers only, while the measured linewidths are influenced, among other things, by instrument linewidth.

RESULTS AND DISCUSSION

Only 1,4-diols can be directly intercalated by replacing water molecules in $\mathrm{VOPO_4 \cdot 2H_2O}$ in a microwave field. Intercalates of other diols had to be prepared by replacing propanol in $\mathrm{VOPO_4 \cdot 2C_3H_7OH}$ with the diols. The intercalates prepared are yellow, well crystalline products. Their diffractograms show the set of the (00*l*) reflections which determine the lattice parameter *c* very precisely. The lattice parameter *a* of the tetragonal cell is determined by a very weak (200) reflection. Other diffraction lines, i.e., (*hk*0) and (*hkl*) were usually not observed. The examples of the diffractograms of the intercalates studied are shown in Fig. 1.

The intercalates of all diols with isostructural $\mathrm{NbOPO_4}$ were similarly prepared by substituting the diol molecules for propanol in $\mathrm{NbOPO_4 \cdot 2C_3H_7OH}$. The intercalates are well crystalline white powders. Besides the set of the (00*l*) lines, their diffractograms usually contain the (110) and (200) reflections (as shown for 1,4-diols in Fig. 2) and only

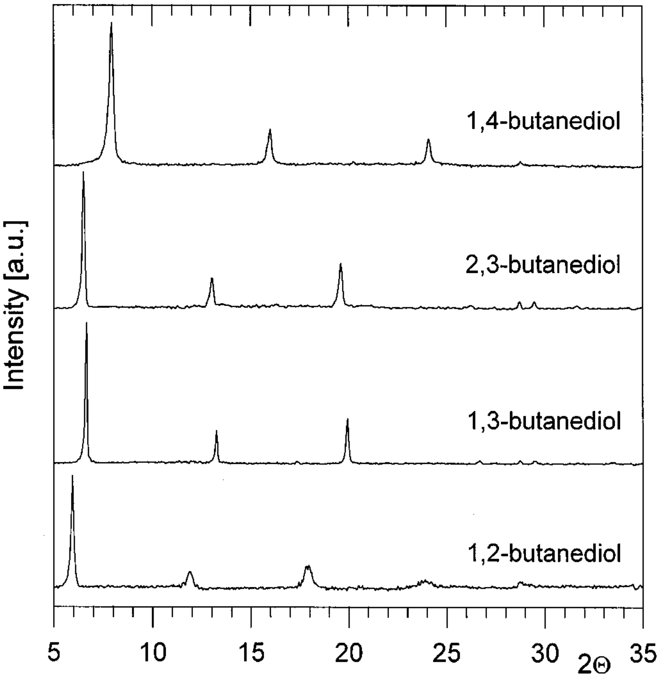

FIG. 1. The diffractograms of the vanadyl phosphate intercalates with saturated C_4 diols.

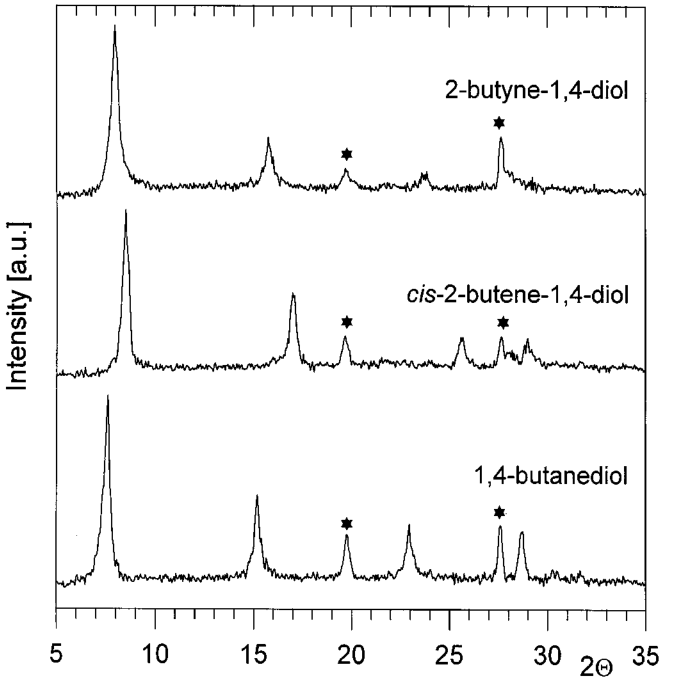

FIG. 2. The diffractograms of the niobyl phosphate intercalates with saturated and unsaturated 1,4-diols. The (*hk*0) lines are indicated by asterisks.

exceptionally the (*hkl*) reflections. The presence of the (*hk*0) and the absence of the (*hkl*) reflections in the diffractograms is characteristic of a turbostratic structure. In this structure, the original tetragonal layers of the hosts are retained but shifted in the directions of the x and/or y axes. The lattice parameters are given in Table 1.

The stoichiometric quotients x_{exp} obtained by the thermogravimetric analysis and several checking analyses of carbon and hydrogen contents are given in Table 1 together with the x_{calc} values calculated as a ratio of the volume of the diol intercalated and the molar volume of the diol which was calculated from its density. The volume of the diol intercalated was calculated as a difference between the unit cell volume of the intercalate and anhydrous $VOPO_4$. As inferred from these results, all the intercalates with 1,4-diols have general formula $MOPO_4 \cdot 1G$ ($M = \mathrm{V, Nb}$; $G =$ 1,4-diol). The 1,2-butanediol intercalates contain about 1.5 guest molecule per formula unit. The 1,3-butanediol and 2,3-butanediol intercalates have probably a little more than one diol molecule per formula unit. Determination of the composition of vanadyl phosphate intercalated with 2,3-butanediol was not possible due to their instability in air. As both starting propanol intercalates—$VOPO_4 \cdot 2C_3H_7OH$ and $NbOPO_4 \cdot 2C_3H_7OH$—do not contain water (2, 8), the presence of water molecules in the interlayer space of all products can be excluded.

TABLE 1
Lattice Parameters and Compositions of the Intercalates of Vanadyl and Niobyl Phosphates with Diols

	$VOPO_4$				$NbOPO_4$			
Diol	a [Å]	c [Å]	x_{exp}	x_{calc}	a [Å]	c [Å]	x_{exp}	x_{calc}
1,2-butanediol	6.21	15.43	1.51	1.46	6.45	15.28	1.55	1.57
2,3-butanediol	6.20	13.51	—	1.21	6.47	13.88	1.25	1.38
1,3-butanediol	6.21	13.39	1.15	1.20	6.46	13.29	1.05	1.30
1,4-butanediol	6.19	11.54	1.05	0.96	6.42	10.83	1.03	0.95
2-butene-1,4-diol	6.16	10.85	1.00	0.95	6.45	10.48	1.06	0.98
2-butyne-1,4-diol	6.22	11.20	1.08	0.94	6.49	11.59	1.00	1.10

The infrared spectra of the intercalates show bands characteristic of alcohol intercalates (9). In the region 3000 to 3500 cm^{-1}, a typical set of broad bands corresponding to OH group vibrations is observed. The widths and positions of the bands are influenced by the mutual interactions of the guest molecules and by the interactions of the OH groups with the lattice of the host. All the intercalates show C-H stretching bands in the 2850 to 2960 cm^{-1} region. In addition, spectra of both intercalates of 1,4-butenediol show a set of bands characteristic of the presence of double bond: $\nu(=\mathrm{C{-}H})$ at 3030 cm^{-1}, $\nu(\mathrm{C{=}C})$ at 1640 cm^{-1}, $\delta(cis\text{-}\mathrm{CH{=}CH})$ at 1420 cm^{-1} and 1255 cm^{-1}. Other bands of the C=C bond are overlapped by host bands. The band of the C≡C valence vibration was not observed in the IR spectra of the corresponding intercalates due to the symmetry of the 2-butyne-1,4-diol molecule.

The spectra of the $VOPO_4$ intercalates contain the $\nu(\mathrm{V{=}O})$ band in the region 1000–1020 cm^{-1}, overlapping the intense bands of the PO_4 tetrahedron (10). This indicates the presence of a donor–acceptor bond between an oxygen atom of the diol and a vanadium atom. For $NbOPO_4$ compounds, the $\nu(\mathrm{Nb{=}O})$ band is completely overlapped by the bands of the PO_4 group.

As shown earlier (1), the 1,4-butanediol molecules are oriented in the $VOPO_4$ intercalate as a monomolecular layer with the chains perpendicular to the host layers. It can be presumed from the found values of the basal spacing that the molecules of *cis*-2-butene-1,4-diol and 2-butyne-1,4-diol are arranged in the same way in the interlayer space. The observed differences in the basal spacings correspond to this idea because the distances of the terminal oxygens calculated from the bond distances and bond angles (11, 12) decrease in an order 1,4-butanediol (6.20 Å) > 2-butyne-1,4-diol (5.75 Å) > *cis*-2-butene-1,4-diol (5.62 Å). On the other hand, the 1,4-butanediol molecules are tilted at an angle of 74° to the host layers in the niobyl phosphate intercalate (2). For the *cis*-2-butene-1,4-diol intercalate, it is presumed that the guest molecules are also tilted to the host layers due to the lower basal spacing of this intercalate. In contrast, the basal spacing found for the 2-butyne-1,4-diol intercalate

(11.59 Å) indicates that the guest molecules are probably perpendicular to the host layers. The molecules of 1,2-butanediol are arranged between the host layers in a bimolecular way with their aliphatic chains tilted at an angle of 70° (3). For 1,3-butanediol and 2,3-butanediol, the basal spacings and contents of the guests in both hosts (see Table 1) suggest a bimolecular deposition of the guest molecules in the intercalates.

In contrast to the intercalates of all 1,4-diols, which are stable in air at ambient humidity for several days to weeks, the 1,2-butanediol intercalates undergo decomposition (i.e., replacing the guests for water to form a hydrate) in tens of minutes. The stability of the 1,3-butanediol intercalates is similar to that of the 1,4-diol intercalates, their diffractograms remain the same after four days. For 2,3-butanediol intercalated $VOPO_4$, a new phase with basal spacing 8.36 Å and composition $VOPO4 \cdot 0.5(2,3\text{-butanediol}) \cdot H_2O$ is formed very quickly (in several minutes) and it is stable for more than one week without any observed formation of $VOPO_4 \cdot 2H_2O$. The diffractograms of both intercalates are given in Fig. 3. On the other hand, 2,3-butanediol intercalated niobyl phosphate changes into trihydrate during several hours.

The stability of 1,ω-diol intercalates in the presence of humidity is most likely given by a pillared arrangement of the guest molecules in the interlayer space of the host. The molecules of 1,4-butanediol, 2-butene-1,4-diol, and 2-butyne-1,4-diol form a monomolecular layer in which every diol molecule is anchored to the both adjacent host layers by the terminal OH groups. Such arrangement is usually more stable than the bimolecular one (found for 1,2-, 2,3-, and 1,3-butanediols) which contains hydrophobic areas of terminal methyl groups in the middle of the interlayer space. The molecules in these areas are held together only by van der Waals forces, hence the interlayer attracting forces are weaker than for the pillared structures. The lowest stability of the 2,3-butanediol intercalate is most likely given by the fact that the terminal methyl groups sterically hinder a closer contact of the hydroxy oxygens with the vanadium atoms of the host layer so that the HO–V bonds are weakened. As follows from our unpublished results (13), the $VOPO_4$ intercalates with 2-alkanols are less stable than the intercalates with 1-alkanols. Unexpected high stability of the intercalate with 1,3-butanediol, which is also arranged in a bimolecular way in the intercalates, is likely given by a system of hydrogen bonds among OH groups placed at the third carbon atom of the alkyl chain. Acidity of the $VOPO_4$ layer is higher than that of the $NbOPO_4$ layer; hence the donor–acceptor bond of the guest molecules to vanadium is stronger than to the niobium atoms in $NbOPO_4$. Therefore the $NbOPO_4$ intercalates are generally less stable against humidity in air at room temperature.

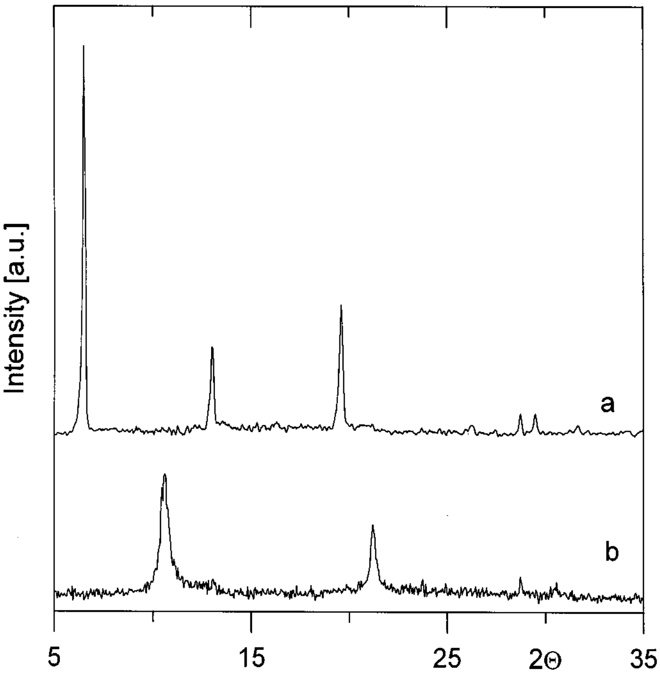

FIG. 3. The diffractograms of 2,3-butandiol intercalated $VOPO_4$ (a) and product of its decomposition in air (b).

The $VOPO_4$ intercalate of 1,4-butanediol forms two phases which coexist in the temperature region from 106 to 130°C (Fig. 4a). Positions and linewidths of the (00*l*) lines are practically unvaried during heating. A similar course of thermal decomposition was observed for $NbOPO_4$ intercalated with 1,4-butanediol and for both hosts intercalated with 2-butene-1,4-diol. As an example, thermal decomposition of $NbOPO_4$ intercalated with 2-butene-1,4-diol is shown in Fig. 5. The basal spacing of the intercalate is almost constant up to 120°C. At 140–160°C, the diol is released from the interlayer space as evident from the steep decrease in the basal spacing. Broad lines of a new phase with basal spacing 8.9 Å are present up to 250°C indicating an arrangement in which two neighboring host layers are bridged by the molecules of the diol. This phase contains about 1/2 molecule of the guest per host formula unit. This type of thermal behavior is typical of all intercalates of $NbOPO_4$ with saturated 1,ω-diols (2). On the other hand, the intercalates of $VOPO_4$ and $NbOPO_4$ with 2-butyne-1,4-diol form amorphous phases at relatively high temperatures of 150 and 175°C, respectively. The intercalates of both hosts with 1,2- and 2,3-butanediols decompose at lower temperatures (about 80 and 60°C, respectively). The $NbOPO_4$ intercalates are generally thermally more stable than the $VOPO_4$ intercalates. The lower thermal stability in the $VOPO_4$ intercalates in comparison with $NbOPO_4$ intercalates is most likely given by reduction of V(V) to V(IV) which is accompanied by decomposition of intercalated alcohols (14). The reduction of V(V) to V(IV) is observed as a change of color of the sample from yellow to green during

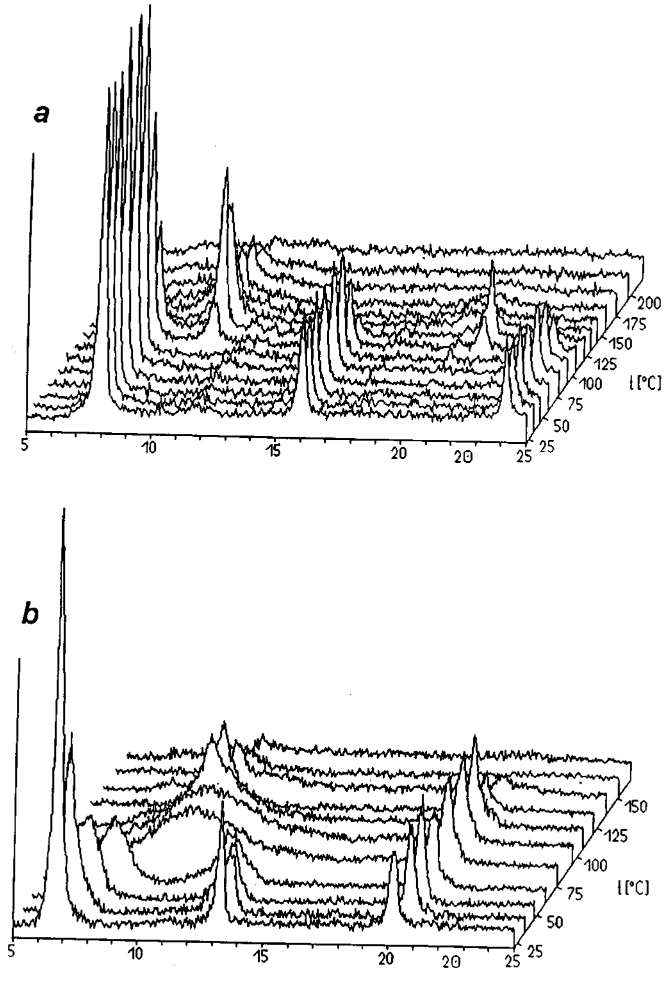

FIG. 4. The changes of the diffractograms during heating of vanadyl phosphate intercalated with 1,4-butanediol (a) and 1,3-butanediol (b).

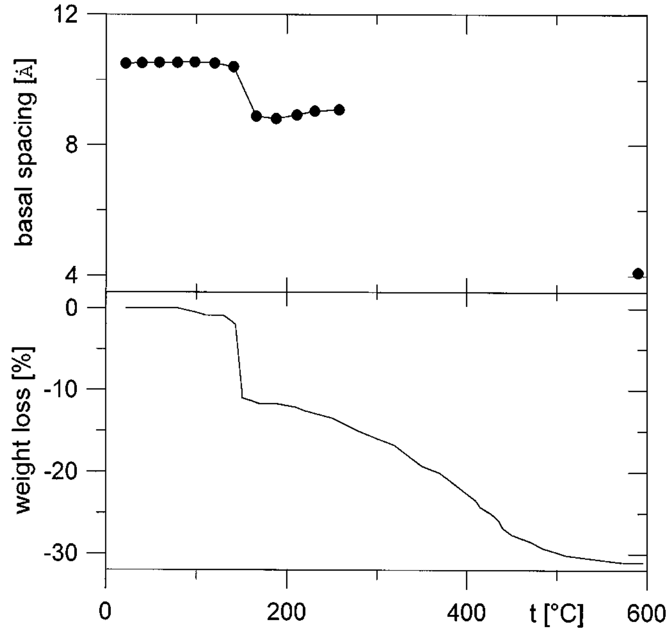

FIG. 5. Thermal decomposition of *cis*-2-butene-1,4-diol intercalated NbOPO$_4$ followed by XRD and thermogravimetry.

heating. Niobium(V) in the analogous niobyl phosphate intercalates is not reduced.

The course of thermal decomposition of VOPO$_4$ intercalated with 1,3-butanediol is different. Changes of the diffractograms during heating this intercalate and 1,4-butanediol intercalated VOPO$_4$ are compared in Fig. 4. On the other hand, the (00*l*) lines of the 1,3-butanediol intercalate are remarkably broaden and their positions are shifted (see Fig. 4b). The broadening of the (00*l*) lines of both phases (parent intercalate: $d_{001} = 13.39$, $d_{002} = 6.70$, and $d_{003} = 4.46$ Å; product formed by heating: $d_{001} = 8.53$ and $d_{002} = 4.27$ Å) can be explained by fragmentation of the microcrystals during heating, nevertheless the shift of the line positions remains unexplained. The behavior described can be elucidated by the formation of a Hendricks–Teller disordered layered lattice (7). We can assume that 1,3-butanediol starts to release from an arbitrary layer of the parent intercalate thus causing liberation of other diol molecules from the same layer. In this way, a random irregular sequence of intercalated and partially deintercalated layers is formed during heating. Thus, we have $d_1 = 13.39$ Å and $d_2 = 8.53$ Å for the Hendricks–Teller function $I_{\mathrm{av}}/|V_{\mathrm{L}}|^2$ in Eqs. [1]–[4]. The fractions f_1 obtained by a nonlinear least-square fitting of the data obtained from the diffractograms measured at various temperatures are given in Table 2. The content of the parent intercalate decreases nearly linearly with increasing temperature in a broad temperature region (more than 80°C). The dependencies of the Hendricks–Teller function on the diffraction angle 2Θ were calculated for the fractions f_1 found. The dependencies of the interplanar distances and linewidths of the (00*l*) lines on temperature (i.e., fraction f_1) calculated by the Hendricks–Teller functions are given in Fig. 6. The calculated values are in a good agreement with

TABLE 2
Content of Parent Intercalated Layers f_1 Calculated from the Hendricks–Teller Function

Temperature [°C]	f_1
34	0.87
46	0.75
60	0.61
75	0.40
93	0.27
107	0.24
120	0.13

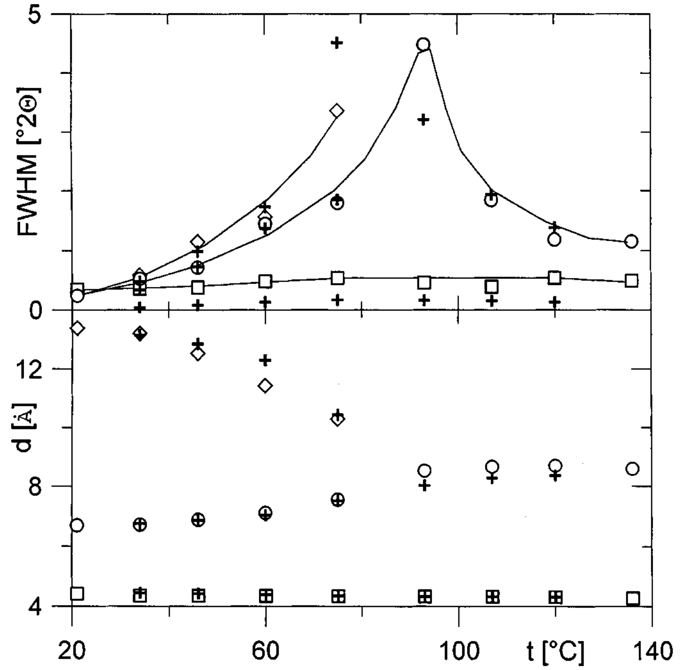

FIG. 6. Dependencies of the interplanar distances *d* and full-widths-at-half-maxima (FWHM) of the (00*l*) diffraction lines of the intercalate of $VOPO_4$ with 1,3-butanediol on temperature (diamonds, circles, and squares—experimental values; crosses—calculated from Hendricks–Teller function).

those obtained from the diffractograms. Considering that the values of d_{003} of the parent intercalate and d_{002} of the product formed by heating are similar, the positions of corresponding diffraction maxima are almost the same and the broadening due to the Hendricks–Teller effect is very small. The difference between observed and calculated linewidths is caused by other factors, e.g., instrumental linewidth and size of crystallites.

ACKNOWLEDGMENTS

This work was supported by the Grant Agency of the Czech Republic (Grant 203/97/1010) and by the Academy of Sciences of the Czech Republic (Key Project 12).

REFERENCES

1. L. Beneš, K. Melánová, V. Zima, J. Kalousová, and J. Votinský, *Inorg. Chem.* **36,** 2850 (1997).
2. L. Beneš, K. Melánová, V. Zima, and J. Votinský, *J. Solid State Chem.* **141,** 64 (1998).
3. K. Melánová, L. Beneš, and V. Zima, *J. Incl. Phenom.* **36,** 301 (2000).
4. G. Ladwig, *Z. Chem.* **19,** 368 (1979).
5. S. Bruque, M. Martinez-Lara, L. Moreno-Real, A. Jimenez-Lopez, B. Casal, and E. Ruiz-Hitzky, *Inorg. Chem.* **26,** 847 (1987).
6. L. Beneš, *Sci. Pap. Univ. Pardubice Ser. A* **2,** 151 (1996); *Chem. Abstr.* **126** (1997) 310616v.
7. S. Hendricks and E. Teller, *J. Chem. Phys.* **10,** 147 (1942).
8. L. Beneš, J. Votinský, J. Kalousová, and J. Klikorka, *Inorg. Chim. Acta* **114,** 47 (1986).
9. G. Socrates, "Infrared Characteristic Group Frequencies," 2nd edn., Wiley, Chichester, 1997.
10. L. Beneš, K. Melánová, M. Trchová, and P. Čapková, P. Matějka, *Eur. J. Inorg. Chem.* 2289 (1999).
11. E. H. Rodd, "Chemistry of Carbon Compounds," Elsevier, Amsterdam, 1964.
12. N. B. Chapman (Ed.), "Aliphatic Compounds," Butterworths, London, 1973.
13. L. Beneš, V. Zima, and K. Melánová, unpublished results.
14. I. J. Ellison, G. J. Hutchings, M. T. Sananes, and J. C. Volta, *J. Chem. Soc. Chem. Commun.* 1093 (1994).